Microwave-assisted reversal of a single electron spin

Cite as: J. Appl. Phys. **125**, 142801 (2019); https://doi.org/10.1063/1.5064593
Submitted: 05 October 2018 . Accepted: 27 March 2019 . Published Online: 10 April 2019

C. Godfrin, S. Lumetti, H. Biard, E. Bonet, S. Klyatskaya, M. Ruben, A. Candini, M. Affronte, W. Wernsdorfer, and F. Balestro

Journal of Applied Physics TUTORIAL scitation.org/journal/jap

Microwave-assisted reversal of a single electron spin

Cite as: J. Appl. Phys. **125**, 142801 (2019); doi: 10.1063/1.5064593
Submitted: 5 October 2018 · Accepted: 27 March 2019 ·
Published Online: 10 April 2019

C. Godfrin,[1] S. Lumetti,[2,3] H. Biard,[1] E. Bonet,[1] S. Klyatskaya,[4] M. Ruben,[4,5] A. Candini,[2,6] M. Affronte,[2,3,a)] W. Wernsdorfer,[1,4,7] and F. Balestro[1,8,a)]

AFFILIATIONS

[1]Université Grenoble Alpes, CNRS, Grenoble INP, Institut Néel, 38000 Grenoble, France
[2]Istituto Nanoscienze–CNR, Centro S3 Modena, via G. Campi 213A, 41124 Modena, Italy
[3]Dipartimento di Scienze Fisiche, Informatiche e Matematiche, Università degli Studi di Modena e Reggio Emilia, via G. Campi 213A, 41124 Modena, Italy
[4]Institute of Nanotechnology, Karlsruhe Institute of Technology (KIT), 76344 Eggenstein-Leopoldshafen, Germany
[5]Institut de Physique et Chimie des Matériaux de Strasbourg, UMR 7504 UdS-CNRS, 67034 Strasbourg Cedex 2, France
[6]Istituto di Sintesi Organica e Fotoreattività (ISOF), Consiglio Nazionale della Ricerca (CNR), Via Gobetti 101, 40129 Bologna, Italy
[7]Physikalisches Institut, Karlsruhe Institute of Technology (KIT), Wolfgang-Gaede-Str. 1, 76131 Karlsruhe, Germany
[8]Institut Universitaire de France, 103 boulevard Saint-Michel, 75005 Paris, France

[a)]**Authors to whom correspondence should be addressed:** marco.affronte@unimore.it and franck.balestro@neel.cnrs.fr

ABSTRACT

The dynamics of a quantum system in a dissipative environment presents a rich and still largely unexplored phenomenology that is relevant for the control of quantum devices. The simplest problem can be modeled as a two-level system—such as a spin—in contact with a thermal bath. Here, we present experiments in which we monitor the spin reversal in a $TbPc_2$ single-molecule spin transistor, and we show that the application of microwave pulses can cause the spin to flip between its two lowest-lying states ($|\uparrow\rangle$ and $|\downarrow\rangle$) at a rate that increases with increasing duration and power of the pulses. This process is neither resonant nor coherent with the microwave pulses. Moreover, an asymmetry appears in the $|\downarrow\rangle \rightarrow |\uparrow\rangle$ and $|\uparrow\rangle \rightarrow |\downarrow\rangle$ transition probabilities, suggesting that the process occurs out of equilibrium. We explain the experimental results and provide an estimate of the local temperature increase induced by the microwave pulses by means of a model that takes into account the energy exchange between the single Tb^{3+} electron spin and the local environment.

Due to their discrete and utterly quantum-mechanical nature, individual spins represent genuine two-level systems. In particular, single electron spins are a natural and attractive choice for atomic-scale devices encoding quantum bits.[1] Addressing single electron spins confined to quantum dots in high-mobility heterostructures has been a widely investigated playground.[2–7] The electrical single-shot readout of the state of an individual electron spin in a semiconductor quantum dot was achieved by converting the spin information into charge information and subsequently probing the charge on the dot by means of quantum point contact detection.[2,3]

The solid-state spin qubit devices carved out in these semiconducting heterostructures are several tens of nanometers in size. An attractive road to improve the spatial resolution in addressing spin centers is the use of scanning tunneling microscopy (STM). Recently, STM-based experiments have indeed demonstrated the possibility to assemble and address the magnetic states of artificial few-atom magnets.[8–10] In particular, spin-polarized STM can measure the orientation of the spin magnetic moment of bistable magnetic nanostructures through a change in the tunnel current due to tunneling magnetoresistance at the single-atom scale.[11] Transitions between their magnetic states can be induced using the spin-polarized STM as a source of spin-polarized current and controlling the sign of the tip-sample voltage.[8,9] An analogous STM-based protocol allowed one to write and read out the

magnetic state of an individual Ho atom deposited on a MgO surface: current pulses are applied to flip the atom's spin (writing process) and tunnel magnetoresistance is exploited to detect its state (readout phase). The information thus encoded in the single Ho atom spin state can be retained over several hours at liquid helium temperatures.[12,13] Finally, using resonant radio-frequency STM, resonant spectroscopy was performed on a single molecular magnet.[14]

Molecular (spin-)electronics—i.e., devices with molecules embedded between nanoscale electrodes[15–17]—provides alternate ways to read individual spins. Since the use of electromigration to fabricate nanometer separation of metallic electrodes,[18] single-molecule transistors have been fabricated, enabling the realization of large charging energy quantum dots, with, in addition, the possibility of tuning the potential of the molecule with a local gate electrode.[19–21] Molecular magnets have also been embedded between nanoscale electrodes, resulting in the readout or control of magnetic properties.[22–25] These molecular spins, consisting of an inner magnetic core with a surrounding shell of organic ligands,[26,27] can be largely tailored via chemical synthesis and optimized to be grafted on surfaces,[28] to enhance their conducting properties or to engineer their coupling to the environment.[29] At low temperatures, compounds of this class exhibit an extremely slow relaxation of the magnetization[30] and long coherence times,[31] which makes them attractive for density information storage and quantum computing applications.[32] Their high versatility makes it easy to integrate them in a wide variety of nanoscale devices.[33–36]

In this work, we report the spin reversal induced by microwave (MW) pulses. We performed low-temperature experiments on the individual electron spin of a bis(phthalocyaninato) terbium molecule (hereafter $TbPc_2$) embedded in a gold nanojunction obtained via electromigration to create a molecular spin transistor device.

Our spin transistor [Fig. 1(a)] can be described as resulting from the coupling between two quantum systems:

1. The magnetic moment of an isolated $TbPc_2$ molecule:[37–39] the electronic structure $[Xe]4f^8$ of the rare earth ion results in a total spin of $S = 3$ and a total orbital angular momentum of $L = 3$, whose combination, due to the strong spin-orbit coupling, gives rise to an electron spin of global angular momentum $J = 6$. This magnetic moment is subject to the ligand field generated by the two neighboring Pc ligands, which lifts the degeneracy between the $|J, m_j\rangle$ states, inducing an energy gap of ~600 K between the ground-state doublet $|6, \pm 6\rangle$ and the first excited state $|6, \pm 5\rangle$. As a consequence, at low temperature, the magnetic properties of this molecular complex are determined exclusively by this electron spin ground-state doublet, and the $TbPc_2$ single-ion magnet can be described as an Isinglike system, with the electronic magnetic moment of the Tb^{3+} ion (hereafter referred to as "spin" for simplicity) aligned either parallel ($|\uparrow\rangle$) or antiparallel ($|\downarrow\rangle$) to the easy axis of magnetization of the molecule which is perpendicular to the Pc planes. A finite external magnetic field can finally lift the degeneracy of the ground-state doublet through the Zeeman effect [Fig. 1(b)]. Moreover, the Tb^{3+} ion also carries a finite nuclear spin of $I = 3/2$. Though, when applying microwave pulses with frequency equals to 2.8 GHz and power at room temperature of a few dBm, as performed in this work, the nuclear spin transitions (2.45 GHz, 3.13 GHz, and 3.81 ± 0.01 GHz), are unaffected by these pulses. As a consequence, the coupling between the global angular momentum and the Tb^{3+} nuclear spin has no influence on the mechanism under investigation here.
2. A readout quantum dot created in close proximity to the Tb^{3+} electron spin by the two organic Pc ligands, whose delocalized π-electron system is tunnel-coupled to the source and drain electrodes. The presence of an unpaired electron delocalized over the Pc ligands as an $S = 1/2$ radical[40,41,42] likely facilitates the formation of a molecular quantum dot in the neutral derivative $[TbPc_2]^0$ used in our experiments. In addition, it has been shown that the anisotropic magnetic moment of the Tb^{3+} ion is coupled to the Pc π orbitals via an indirect exchange coupling mediated by the 5d electrons of Tb.[29]

The Tb^{3+} electron spin can reverse following two different mechanisms [see the Zeeman diagram in Fig. 1(b)]. At zero magnetic field, quantum tunneling of the magnetization (QTM) can occur, due to the transverse terms of the magnetic anisotropy mixing the two states of the lowest doublet,[39] as illustrated in the inset of Fig. 1(b). The effects of QTM during field sweep across zero were studied and reported in our previous work.[43] At finite magnetic fields (applied parallel to the easy axis of the molecular magnet), the Tb^{3+} electron spin can flip through an exchange of energy and momentum with the environment occurring via the inelastic emission or absorption of one phonon matching the Zeeman energy splitting [direct transition (DT)] or by means of higher-order processes involving two phonons.[26]

The electronic readout of the electron spin orientation uses the exchange coupling between the readout quantum dot formed by the Pc ligands and the Tb^{3+} electron spin, as presented in our previous work.[44] To summarize the readout principle, the chemical potential of the readout dot takes on slightly different values according to whether the Tb^{3+} magnetic moment is aligned parallel or antiparallel to the unpaired electron spin of the readout quantum dot. As a result, by choosing a gate voltage working point close to a charge degeneracy point, a slight variation of the readout quantum dot chemical potential variation results in a relatively high differential conductance variation. Thus, the conductance through the molecular quantum dot is Tb^{3+} electron spin-dependent, allowing for an electrical and nondestructive readout of the electron spin.[28] Indeed, the two electron spin states are associated with two different conductance values and a spin reversal results in a well-defined change in the conductance of about 4%. The observation of these well-defined jumps in the conductance of our molecular spin transistor is well visualized in Fig. 2.

In order to properly choose the time scales involved in the electron spin manipulation experiments, we preliminarily evaluated its lifetime by means of the following measurement protocol. Firstly, the Tb^{3+} electron spin was initialized in its ground state by applying a negative parallel magnetic field $B = -60$ mT. Then, the magnetic field was swept at a rate of 100 mT/s up to $B_0 = 60$ mT, so as to prepare the electron spin in its excited state (if a QTM event occurred before reaching B_0, *vide infra*, the initialization procedure was repeated). Finally, the waiting time necessary for the electron

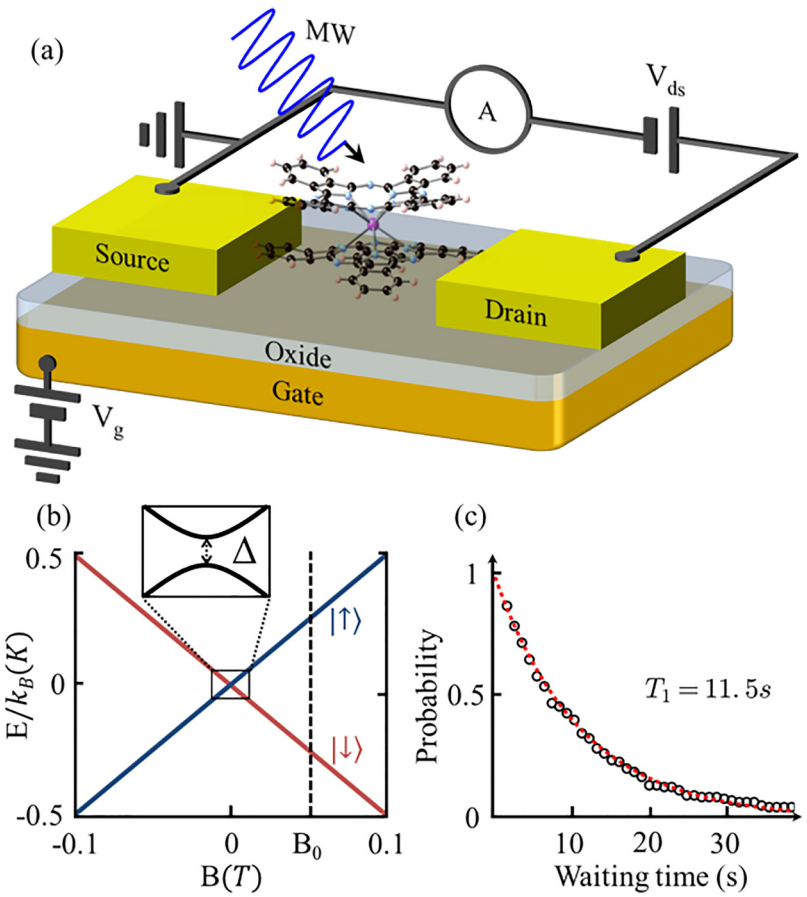

FIG. 1. (a) Schematic illustration of the three-terminal molecular spin transistor consisting of an individual $TbPc_2$ single-ion magnet inserted in a nanometer-sized gold junction obtained by electromigration. A local backgate electrode is located under the molecular junction and separated from the source and drain terminals by an 8-nm-thick oxide layer. The measurement circuit is also represented in the picture. (b) Zeeman diagram of the $TbPc_2$ molecular magnet, showing the energy of the electronic spin levels as a function of the external magnetic field applied parallel to the easy axis of magnetization. We do not consider, in the Zeeman diagram, the coupling between this electronic spin and the Tb^{3+} nuclear spin, as it is not relevant to the mechanism under investigation in this work. At zero magnetic field, the Tb^{3+} electronic spin can reverse its orientation through quantum tunneling of magnetization (QTM) at the avoided level crossing (see inset) induced by the ligand field, whereas phonon-mediated relaxation processes (Direct Transitions, DT) can occur at finite fields B_0. (c) Electronic spin lifetime (black circles) plotted as the probability to find the system in its initial state after a certain waiting time t for a parallel magnetic field $B_0 = 60$ mT and a temperature $T = 40$ mK. The red dotted line represents a fit of the experimental data to the function $\exp(-t/T_1)$, from which a relaxation time $T_1 = 11.5$ s can be extracted.

spin to relax into its ground state—thus reversing its orientation—was recorded. This measurement scheme was iterated 200 times and the waiting times were collected yielding the probability to find the system in the initial state [see Fig. 1(c)]. By fitting the experimental data (black circles) with a simple exponential decay function of the type $e^{-\frac{t}{T_1}}$ (red dotted line), a relaxation time of $T_1 = 11.5$ s for the Tb^{3+} electron spin was estimated.

In the following, we focus on low-temperature experiments maintaining the external (parallel) magnetic field at a fixed finite value of $B_0 = 60$ mT, which leaves the DT as the only possible mechanism for the spin reversal. If the system is kept at equilibrium in these conditions ($T = 40$ mK, $B_0 = 60$ mT), it will exhibit a constant conductance corresponding to the electron spin state $|\downarrow\rangle$, as depicted in the first half of the time trace reported in Fig. 2(c). This is not surprising, since in these experimental conditions, the $|\downarrow\rangle$ state is energetically favored [see the Zeeman diagram in Fig. 1(b)] and, with no external stimuli acting on the spin system, the Tb^{3+} electron spin remains in its ground state. The situation changes if the application of MW pulses is included in the experiment. For this, we followed the *probe-pulse-probe* protocol schematized in Fig. 2(a). First, the molecular spin transistor conductance is measured over a time window $\tau_m = 0.4$ s (much shorter than the electron spin relaxation time T_1 estimated above). Subsequently, a microwave pulse of duration τ_P and power P, estimated at the dilution refrigerator input, is applied through an antenna located in close proximity to the device. This antenna is capacitively coupled to the source-drain transistor, resulting in a MW electric excitation in the nanogap where the molecular magnet is embedded. Finally, after a total waiting time $\tau_w = 0.1$ s (required by our data acquisition electronics), a new conductance measurement is started, in order to probe the resulting electron spin state. When this sequence is repeated continuously, a bistable time trace is observed, with the conductance switching between two well-defined values corresponding to the two quantum states of the Tb^{3+} electron spin, as displayed in the second half of the conductance time trace illustrated in Fig. 2(c) (where vertical dotted lines are put on the graph whenever a microwave pulse is applied).

The *probe-pulse-probe* protocol was iterated a few hundreds of times in order to gather significant statistics. For each MW pulse sent to the spin device, the difference Δg between the conductance measured after the pulse and the conductance measured before the pulse was computed and different events were discerned. The histogram in Fig. 2(b) shows the final distribution of the Δg values. Three well-separated peaks can be discriminated, which are respectively centered at (i) $\Delta g = -35$ nS ($\Delta g/g \sim 4\%$), corresponding to spin flip events from the $|\uparrow\rangle$ to the $|\downarrow\rangle$ electron spin state (peak #1);

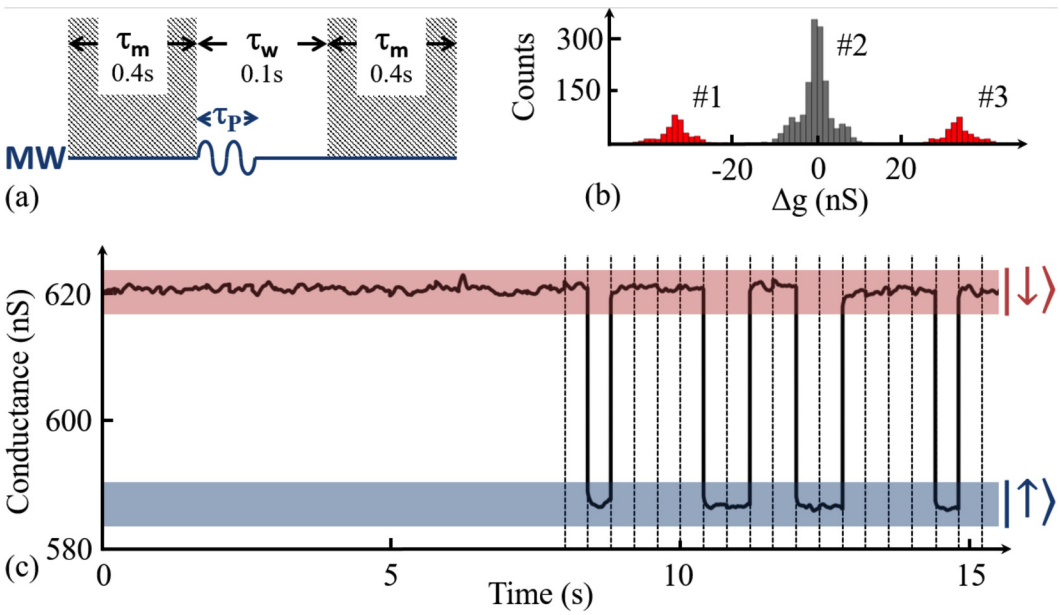

FIG. 2. (a) Scheme of the measurement protocol used to probe the effect of MW pulses on the electron spin state of the $TbPc_2$ single-ion magnet. The device conductance is measured for a time interval $\tau_m = 0.4$ s before and after the application of a MW pulse of duration τ_P and power P. A time $\tau_w = 0.1$ s is awaited before starting the conductance measurement after the application of the pulse. A constant external parallel magnetic field $B_0 = 60$ mT is applied during the entire procedure. (b) Histogram of the difference Δg between the conductance measured after and before the application of each MW pulse. The two lateral peaks (#1 and #3) correspond to reversals of the electron spin, while the central one (#2) collects events in which no electron spin flip was observed as an effect of the MW pulses. (c) Evolution of the device conductance as a function of time at a constant parallel magnetic field $B_0 = 60$ mT. MW pulses (indicated on the plot as vertical dotted lines) are applied to the spin transistor only in the right half of the time trace.

(ii) $\Delta g = 0$ nS, where no reversal of the electron spin has taken place (peak #2); and (iii) $\Delta g = +35$ nS, corresponding to transitions from the $|\downarrow\rangle$ to the $|\uparrow\rangle$ state (peak #3). This result demonstrates that it is therefore possible to induce transitions between the electron spin states by applying MW pulses of proper duration and amplitude at a constant parallel magnetic field. We can define the probability for the electron spin reversal to be induced by the MW pulses as

$$\text{Probability} = \frac{N_1 + N_3}{N_1 + N_2 + N_3},$$

with N_i being the number of events included in the ith peak ($i = 1$, 2, 3). The evolution of the spin flip probability was investigated by varying the MW pulse parameters. A systematic change of the frequency between 2.3 and 6 GHz did not show any significant resonance with our spin system. This is not surprising since electron paramagnetic resonance (EPR) transitions between the $|+6\rangle$ and $|-6\rangle$ states—involving 12-photon processes—are strongly improbable. In the following, we set $f = 2.8$ GHz. For a fixed MW pulse duration $\tau_P = 2\,\mu$s, the probability to reverse the Tb^{3+} electron spin is essentially zero for pulse powers P up to about 2.5 mW, as depicted in Fig. 3(b). For higher values of P, the probability of the spin reversal process increases for increasing pulse power, attaining a maximum value of approximately 0.3. Analogously, the spin flip probability was also measured as a function of the MW pulse duration τ_P for pulses of power $P = 10$ mW. As shown in Fig. 3(a), the spin reversal probability increases for increasing pulse lengths in the submicrosecond regime and subsequently achieves a plateau, remaining almost constant around 0.3 up to $\tau_P = 2\,\mu$s. It is worth noting that no oscillations of the probability as a function of τ can be observed: this implies that the MW-induced spin reversal process is not coherent.

Figure 3(c) features the behavior of the spin reversal probability as a function of the external magnetic field applied parallel to the easy axis of magnetization of the $TbPc_2$ single-ion magnet. The probability is independent of the value chosen for B_0, further confirming that the electron spin reversal process is not resonant with the MW pulses: the interaction between the Tb^{3+} electron spin and the MW electromagnetic field must be mediated by some additional mechanisms. To interpret these results, we consider a phenomenological picture in which the MW pulses induce a local temperature increase of the experimental system, thus exciting the local environment that subsequently relaxes by exchanging energy and momentum with the Tb^{3+} electron spin, causing it to reverse its orientation. It is not trivial to precisely assess the temperature of the system induced by the application of the MW pulses. Nonetheless, we can exclude that T rises higher than 20–30 K, above which we know that irreversible modifications of the molecular device are likely to occur.

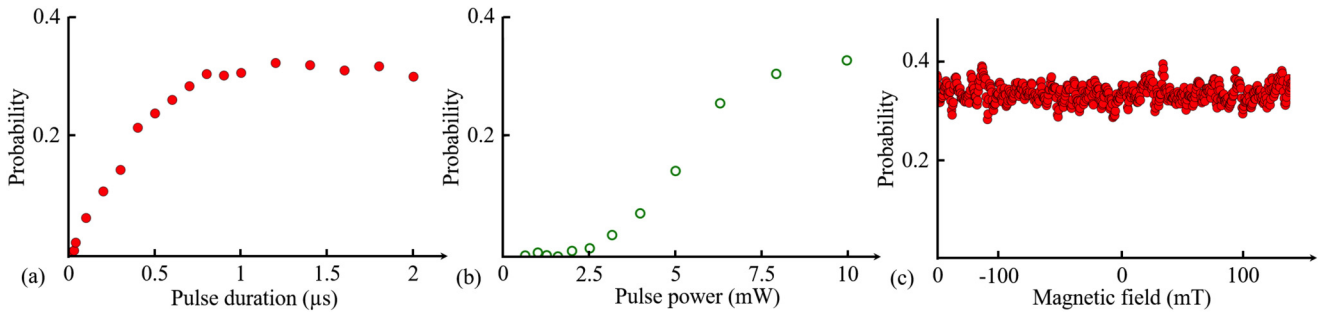

FIG. 3. (a) Probability of the MW-induced spin reversal process as a function of the MW pulse duration τ_P with $P = 10$ mW. Pulses longer than $2\,\mu$s were not applied in order to preserve the integrity of the sample. (b) Probability of the MW-induced spin reversal process as a function of the MW pulse power P with $\tau_P = 2\,\mu$s. Pulses more powerful than 10 mW were not applied in order to preserve the integrity of the sample. (c) Probability of the MW-induced spin reversal process as a function of the external magnetic field applied parallel to the easy axis of magnetization of the $TbPc_2$ molecular magnet for MW pulses of power $P = 10$ mW and duration $\tau_P = 2\,\mu$s. No significant dependence is observed.

To provide an order-of-magnitude assessment, we considered the spin-lattice relaxation model reported in Abragam *et al.*[45] in which the relaxation time τ_1 of a two-level spin system due to phonon-assisted processes is derived as a function of the temperature T of the phonon bath with which the spin system is in thermal contact. The model relies on the theory of spin-lattice relaxation through modulation of the ligand field induced by lattice vibrations[46–48] and takes into account the phonon density of a three-dimensional crystal at equilibrium. Applying this model to our molecular spin device, we find that the relaxation time goes as

$$\frac{1}{\tau_1} = \underbrace{\alpha \coth\left(\frac{\hbar\omega}{2k_BT}\right)}_{\text{Direct}} + \underbrace{aT^7 + b}_{\text{Raman}} + \underbrace{\tau_0^{-1}\exp\left(-\frac{\Delta}{k_BT}\right)}_{\text{Orbach}}.$$

The various terms originate from different processes that contribute simultaneously (but in a widely varying degree) to the relaxation rate:

1. The first term refers to the DT process, involving phonons having the same energy as the $\hbar\omega$ splitting between the two states of the spin system. In the formula, k_B is the Boltzmann constant and the $\alpha = 0.09\,s^{-1}$ prefactor was calculated knowing the energy splitting $\hbar\omega = 2.8$ GHz ~ 140 mK between the spin $|\uparrow\rangle$ and spin $|\downarrow\rangle$ states induced by the external parallel magnetic field $B_0 = 60$ mT and the electron spin lifetime $T_1 = 11.5$ s [Fig. 1(c)] when the temperature of the phonon bath is the same as the temperature of the dilution cryostat ($T = 40$ mK).
2. The second term describes the Raman process, a two-phonon mechanism involving the virtual absorption of a phonon of energy $\hbar\omega_1$ followed by the emission of a phonon of energy $\hbar\omega_2$ such that $\hbar\omega_2 - \hbar\omega_1 = \hbar\omega$. For the parameters a and b, we used the values inferred by Urdampilleta[49] from measurements performed on a similar molecular device: $a = 20\,s^{-1}K^{-7}$, $b = 0.01\,s^{-1}$.
3. The third term refers to the Orbach process, analogous to the Raman mechanism but involving a real excited state instead of a virtual one. The symbol Δ indicates the energy difference between the ground-state doublet and the excited state concerned by the relaxation event. Since for our molecular system $\Delta \sim 600$ K, at the temperature scales involved in our experiments, the contribution of this process can be safely ignored.

Within this approximated model, we can estimate that the temperature required to have a spin lifetime $\tau_1 \sim 1\,\mu$s (corresponding to the pulse duration at which both the transition probabilities start to saturate) is of the order of $T \sim 5$ K, which is likely to be the order-of-magnitude temperature of the system during the application of the MW pulse (i.e., during τ_P). Moreover, although indirectly, we can estimate the system temperature during the conductance measurements by considering the direct relaxation events observed in the corresponding $\tau_m = 0.4$ s time windows, their number is compatible with a temperature $T \sim 50$ mK (very close to the dilution fridge temperature).

To learn more on the physical processes involved in the MW-induced reversal of the Tb^{3+} electron spin, we separately evaluated the switching probabilities q_{ij} referred to the $|\downarrow\rangle \rightarrow |\uparrow\rangle$ and to the $|\uparrow\rangle \rightarrow |\downarrow\rangle$ transitions as $q_{ij} = n_{ij}/n_i$, where n_{ij} is the number of transitions from state i to state j (with $i, j = |\uparrow\rangle, |\downarrow\rangle$) and n_i is the number of pulses starting in state i.[8] Figures 4(a) and 4(b) show how these transition probabilities evolve as a function of the pulse power P (at constant $\tau_P = 2\,\mu$s) and of the pulse length τ_P (at constant $P = 10$ mW), respectively. Probabilities referred to the transition from the $|\uparrow\rangle$ to the $|\downarrow\rangle$ electron spin state are represented by filled red circles, while probabilities related to the transition from the $|\downarrow\rangle$ to the $|\uparrow\rangle$ state are drawn as unfilled green dots. We can recognize two main features. On the one hand, an increase of the transition probabilities is observed both for increasing MW pulse power and for increasing pulse duration. This provides additional support to the phenomenological description given above, since an augmentation of the local temperature—which will be higher the longer and/or the more powerful the applied MW pulses—is expected to reduce the lifetime of both electron spin states, thus increasing the probability to switch the spin from one state to the other. On the other hand, both graphs point out the existence of an asymmetry between the $|\downarrow\rangle \rightarrow |\uparrow\rangle$ and $|\uparrow\rangle \rightarrow |\downarrow\rangle$ transitions.

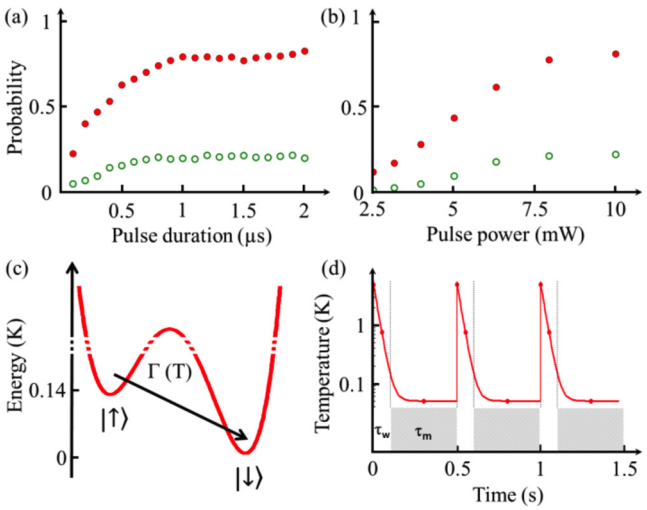

FIG. 4. Transition probabilities as a function of the MW pulse duration τ_P with $P = 10$ mW (a) and as a function of the pulse power P with $\tau_P = 2\,\mu$s (b). In both graphs, filled red dots are referred to the $|\uparrow\rightarrow|\downarrow$ transition, whereas unfilled green circles are related to the $|\downarrow\rightarrow|\uparrow$ spin transition. (c) Asymmetric double-well potential picturing the energy of the Tb^{3+} electron spin states as induced by the external parallel magnetic field $B_0 = 60$ mT. The MW pulses excite the spin system that can then relax in either state with equal probability. When the spin falls in the $|\uparrow$ state well, it can flip to the $|\downarrow$ state via a direct relaxation mechanism. Our protocol of measurement is "blind" to the direct relaxation events taking place in the $\tau_w = 0.1$ s time window that foreruns the beginning of a new conductance measurement: these events account for the asymmetry in the $|\uparrow\rightarrow|\downarrow$ and $|\downarrow\rightarrow|\uparrow$ transition probabilities. (d) Evolution of the local temperature of the system during the different phases of our probe-pulse-probe protocol: application of a MW pulse during τ_P (not explicitly reported on the graph for scale reasons), waiting time τ_w, and conductance measurement during τ_m. The plot includes three consecutive MW pulses which are sent to the system at $t = 0$, $t = 0.5$ s, and $t = 1.0$ s, respectively. The red dots indicate the average local temperatures estimated for the three measurement stages using our spin-lattice relaxation model: $T = 5$ K during τ_P, $T = 750$ mK during τ_w, and $T = 50$ mK during τ_m. The red line fits these points assuming that, after the MW pulse, the temperature relaxes following an exponential decay $y_0 + A\exp(-bt)$, where t is the time.

This asymmetry is also evident from the bistable time trace in Fig. 2(c), where it is apparent that switching from the $|\uparrow$ to the $|\downarrow$ state requires, on an average, the application of a smaller number of pulses than reversing the electron spin from the $|\downarrow$ to the $|\uparrow$ state. Figures 4(a) and 4(b) show that the difference between the actual $|\uparrow\rightarrow|\downarrow$ and $|\downarrow\rightarrow|\uparrow$ transition probabilities increases for increasing pulse power and duration, attaining a constant value for pulse powers higher than 7.5 mW and pulse durations longer than $1\,\mu$s. In particular, in this regime, the $|\uparrow\rightarrow|\downarrow$ transition probability is about 0.8, while the probability related to the opposite transition is approximately equal to 0.2.

The asymmetry in the transition probabilities—which evidences that the process occurs out of equilibrium—can be explained by taking into account the fact that, after the application of a microwave pulse, a time $\tau_w = 0.1$ s is awaited before performing a new conductance measurement [Fig. 2(a)]: during this interval, imposed by the electronic setup, we are "blind" to any possible electron spin reversal. It is likely that during τ_w, the Tb^{3+} electron spin relaxes back to the $|\downarrow$ state (i.e., the ground state) via a direct relaxation process. As a consequence, no effective change in the conductance is observed for these events after the application of the pulse, and hence a certain number of MW-induced $|\downarrow\rightarrow|\uparrow$ transitions are actually missed. This leads to an overestimation of the $|\uparrow\rightarrow|\downarrow$ transition probability with a consequent underestimation of the $|\downarrow\rightarrow|\uparrow$ probability. Note that if the transistor conductance could be recorded in real time over the entire measurement window (i.e., no waiting time τ_w involved), all of the direct relaxation events flipping the electron spin from the $|\uparrow$ to the $|\downarrow$ state would be detected and, as a result, symmetric transition probabilities would be observed.

Considering this hypothesis, we expect that the relaxation events taking place in the $\tau_w = 0.1$ s time window before the start of the new conductance measurement occur roughly 30% of the times, in order to set equal the $|\uparrow\rightarrow|\downarrow$ and $|\downarrow\rightarrow|\uparrow$ transition probabilities displayed in Figs. 4(a) and 4(b) in the high power and long pulse regime. Using an exponential decay function $P(t) = 1 - \exp(-t/\tau_1)$ to describe the probability for the relaxation process to occur as a function of time, requiring $P(t_w = 0.1\,\text{s}) = 0.3$, we get $\tau_1 = -(0.1\,\text{s})/\ln 0.7 = 0.28$ s and a consequent value for the temperature of $T \sim 750$ mK. This can be considered the average temperature of the environment during the waiting time.

We also remark that the increase of the difference between the $|\uparrow\rightarrow|\downarrow$ and $|\downarrow\rightarrow|\uparrow$ transition probabilities with increasing duration/power of the pulse agrees well with our picture of a further relaxation toward the ground state occurring during τ_w.

Figure 4(d) summarizes the temporal evolution of the local temperature of the system during the various stages of the measurement resulting from the application of the MW pulses followed by a thermal relaxation of the environment.

The phenomenological picture that stems from all the previous discussions is schematized in Fig. 4(c), where an asymmetric double-well potential is used to describe the Tb^{3+} electron spin system (the asymmetry being due to the presence of the finite parallel magnetic field $B_0 = 60$ mT, which makes the $|\downarrow$ spin state energetically favorable). The application of the MW pulses causes an increase in the temperature of the phonon bath, which in turn relaxes back to equilibrium by exchanging energy and momentum with the Tb^{3+} electron spin. The electron spin is provided in this manner with an amount of energy higher than the energy of the bottom of both the potential wells and can relax in either of them with equal probability, as the process is thermally induced and thus incoherent by definition. Finally, when the electron spin goes in the $|\uparrow$ state, it can switch back to the $|\downarrow$ spin state via a relaxation mechanism occurring during the $\tau_w = 0.1$ s time interval which is awaited for before starting a new conductance measurement. This happens with a probability that depends on the temperature increase induced by the MW pulses and accounts for the observed asymmetry in the measured $|\uparrow\rightarrow|\downarrow$ and $|\downarrow\rightarrow|\uparrow$ transition probabilities.

We remark that our model relies on quite simple assumptions, as it computes the spin-lattice relaxation time by considering a three-dimensional phonon density at thermal equilibrium. We believe that these experiments may inspire a more accurate and

comprehensive model that can properly describe the dynamics of a single spin in contact with a local bath whose temperature can be changed by the application of MW pulses. An appropriate theoretical treatment—beyond the scope of this work—will probably require to solve a master equation for the density matrix describing the spin and the local environment. As for the (bosonic) phonon bath, a low-dimensional phonon density of states should be better used to describe our system. The effects of additional contributions (so far neglected) will be possibly taken into account, for instance, the role played by the molecule's organic radical and by the (fermionic) bath of conduction electrons tunneling across the quantum dot.

In conclusion, we showed the possibility to address and switch, by means of MW pulses, the electron spin carried by an individual $TbPc_2$ single-ion magnet in a single-molecule transistor configuration. The probability of the spin reversal process, being nonresonant with the MW pulses, increases with increasing pulse duration and power (namely, with increasing microwave field energy) and achieves saturation already for pulse durations of $\sim 1\,\mu s$, meaning that the spin switching can be performed at megahertz frequencies. The experimental results can be understood by considering that the Tb^{3+} electron spin reverses its orientation because of energy exchange with the phonon bath located in its surroundings and heated up by the application of the MW pulses. We estimated an order of magnitude of the average temperature of the local environment during the different stages of the probe-pulse-probe measurement protocol following the application of the MW pulses. Yet, the observed asymmetry in the spin reversal process (between $|\uparrow\rightarrow|\downarrow$ and $|\downarrow\rightarrow|\uparrow$ transitions) indicates that the process occurs out of equilibrium and its description asks for a more sophisticate modeling that goes beyond the scope of this work. The possibility to read and write the spin information on individual molecules in a transistor geometry is a step forward in the context of the manipulation of an individual electron spin carried by a single molecular magnet. It will be relevant for the developments of future molecular devices, including local temperature sensors, memories, spintronics, and quantum applications.

This work is partially supported by the MolSpin COST Action 15128, by the French National Agency of Research through the ANR-13-BS10-0001 MolQuSpin, by the European Community through the FET-Proactive Project MoQuaS (Contract No. 610449), by the German Research Foundation (DFG) through the Transregio Project No. TR88 3MET, by the Alexander von Humboldt Foundation, and by the Italian Ministry for Research (MIUR) through the FIR Grant No. RBFR13YKWX. The samples were fabricated at the NANOFAB facility of the Néel Institute. The authors acknowledge the fruitful collaboration with E. Eyraud, Y. Deschanels, D. Lepoittevin, C. Hoarau, and C. Thirion for experimental setup and software development.

REFERENCES

[1]D. Loss and D. P. DiVincenzo, "Quantum computation with quantum dots," Phys. Rev. A **57**, 120–126 (1998).
[2]J. M. Elzerman, R. Hanson, L. H. Willems van Beveren, B. Witkamp, L. M. K. Vandersypen, and L. P. Kouwenhoven, "Single-shot read-out of an individual electron spin in a quantum dot," Nature **430**, 431–435 (2004).
[3]R. Hanson, L. H. Willems van Beveren, I. T. Vink, J. M. Elzerman, W. J. M. Naber, F. H. L. Koppens, L. P. Kouwenhoven, and L. M. K. Vandersypen, "Single-shot readout of electron spin states in a quantum dot using spin-dependant tunnel rates," Phys. Rev. Lett. **94**, 196802 (2005).
[4]A. C. Johnson, J. R. Petta, J. M. Taylor, A. Yacoby, M. D. Lukin, C. M. Marcus, M. P. Hanson, and A. C. Gossard, "Triplet-singlet spin relaxation via nuclei in a double quantum dot," Nature **435**, 925–928 (2005).
[5]J. R. Petta, A. C. Johnson, J. M. Taylor, E. A. Laird, A. Yacoby, M. D. Lukin, C. M. Marcus, M. P. Hanson, and A. C. Gossard, "Coherent manipulation of coupled electron spins in semiconductor quantum dots," Science **309**, 2180–2184 (2005).
[6]F. H. L. Koppens, C. Buizert, K. J. Tielrooij, I. T. Vink, K. C. Nowack, T. Meunier, L. P. Kouwenhoven, and L. M. K. Vandersypen, "Driven coherent oscillations of a single electron spin in a quantum dot," Nature **442**, 766–771 (2006).
[7]K. C. Nowack, F. H. L. Koppens, Y. V. Nazarov, and L. M. K. Vandersypen, "Coherent control of a single electron spin with electric fields," Science **318**, 1430–1433 (2007).
[8]S. Loth, S. Baumann, C. P. Lutz, D. M. Eigler, and A. J. Heinrich, "Bistability in atomic-scale antiferromagnets," Science **335**, 196–199 (2012).
[9]A. A. Khajetoorians, B. Baxevanis, C. Hübner, T. Schlenk, S. Krause, T. O. Wehling, S. Lounis, A. Lichtenstein, D. Pfannkuche, J. Wiebe, and R. Wiesendanger, "Current-driven spin dynamics of artificially constructed quantum magnets," Science **339**, 55–59 (2013).
[10]S. Baumann, W. Paul, T. Choi, C. P. Lutz, A. Ardavan, and A. J. Heinrich, "Electron paramagnetic resonance of individual atoms on a surface," Science **350**, 417–420 (2015).
[11]S. Loth, C. P. Lutz, and A. J. Heinrich, "Spin-polarized spin excitation spectroscopy," New J. Phys. **12**, 125021 (2010).
[12]F. D. Natterer, K. Yang, W. Paul, P. Willke, T. Choi, T. Greber, A. J. Heinrich, and C. P. Lutz, "Reading and writing single-atom magnets," Nature **543**, 226–228 (2017).
[13]T. Choi, W. Paul, S. Rolf-Pissarczyk, A. J. Macdonald, F. D. Natterer, K. Yang, P. Willke, C. P. Lutz, and A. J. Heinrich, "Atomic-scale sensing of the magnetic dipolar field from single atoms," Nat. Nanotechnol. **12**, 420–424 (2017).
[14]S. Müllegger, S. Tebi, A. K. Das, W. Schöfberger, F. Fasschinger, and R. Koch, "Radio frequency scanning tunneling spectroscopy for single-molecule spin resonance," Phys. Rev. Lett. **113**, 133001 (2014).
[15]S. Sanvito, "Molecular spintronics," Chem. Soc. Rev. **40**, 3336–3355 (2011).
[16]L. Bogani and W. Wernsdorfer, "Molecular spintronics using single-molecule magnets," Nat. Mater. **7**, 179–186 (2008).
[17]W. Wernsdorfer, "Molecular nanomagnets: Towards molecular spintronics," Int. J. Nanotechnol. **7**, 497–522 (2010).
[18]H. Park, A. K. L. Lim, and A. P. Alivisatos, "Fabrication of metallic electrodes with nanometer separation by electromigration," App. Phys. Lett. **75**, 301–303 (1999).
[19]H. Park, J. Park, A. K. L. Lim, E. H. Anderson, A. P. Alivisatos, and P. L. McEuen, "Nanomechanical oscillations in a single-C_{60} transistor," Nature **407**, 57–60 (2000).
[20]J. Park, A. N. Pasupathy, J. I. Goldsmith, C. Chang, Y. Yaish, J. R. Petta, M. Rinkoski, J. P. Sethna, H. D. Abruña, P. L. McEuen, and D. C. Ralph, "Coulomb blockade and the Kondo effect in single-atom transistors," Nature **417**, 722–725 (2002).
[21]W. J. Liang, M. P. Shores, M. Bockrath, J. R. Long, and H. Park, "Kondo resonance in a single-molecule transistor," Nature **417**, 725–729 (2002).
[22]H. B. Heersche, Z. de Groot, J. A. Folk, H. S. van der Zant, C. Romeike, M. R. Wegewijs, L. Zobbi, D. Barreca, E. Tondello, and A. Cornia, "Electron transport through single Mn_{12} molecular magnets," Phys. Rev. Lett. **96**, 206801 (2006).
[23]M. H. Jo, J. E. Grose, K. Baheti, M. M. Desmukh, J. J. Sokol, E. M. Rumberger, D. N. Hendrickson, J. R. Long, H. Park, and D. C. Ralph, "Signatures of molecular magnetism in single-molecule transport spectroscopy," Nano Lett. **6**, 2014–2020 (2006).

[24]A. S. Zyazin, J. W. G. van den Berg, E. A. Osorio, H. S. J. van der Zant, N. P. Konstantinidis, M. Leijnse, M. R. Wegewijs, W. Hofstetter, C. Danieli, and A. Cornia, "Electric field controlled magnetic anisotropy in a single molecule," Nano Lett. **10**, 3307–3311 (2010).
[25]R. Vincent, S. Klyatskaya, M. Ruben, W. Wernsdorfer, and F. Balestro, "Electronic read-out of a single nuclear spin using a molecular spin transistor," Nature **488**, 357–360 (2012).
[26]D. Gatteschi, R. Sessoli, and J. Villain, *Molecular Nanomagnets* (Oxford University Press, 2006), ISBN: 9780198567530
[27]W. Wernsdorfer, "Molecular nanomagnets: Towards molecular spintronics," Int. J. Nanotechnol. **7**, 497–522 (2010).
[28]A. Cornia, D. R. Talham, and M. Affronte, "Thin layers of molecular magnets," in *Molecular Magnetic Materials: Concepts and Applications*, edited by B. Sieklucka and D. Pinkowicz (Wiley-VCH Verlag GmbH & Co. KGaA, Weinheim, Germany).
[29]A. Candini, D. Klar, S. Marocchi, V. Corradini, R. Biagi, V. De Renzi, U. del Pennino, F. Troiani, V. Bellini, S. Klyatskaya, M. Ruben, K. Kummer, N. B. Brookes, H. Huang, A. Soncini, H. Wende, and M. Affronte, "Spin-communication channels between Ln(III) bis-phthalocyanines molecular nanomagnets and a magnetic substrate," Sci. Rep. **6**, 21740 (2016).
[30]C. Milios, A. Vinslava, W. Wernsdorfer, S. Moggach, S. Parsons, S. Perlepes, G. Christou, and E. Brechin, "A record anisotropy barrier for a single-molecule magnet," J. Am. Chem. Soc. **129**, 2754–2755 (2007).
[31]A. Ghirri, A. Candini, and M. Affronte, "Molecular spins in the context of quantum technologies," Magnetochemistry **3**(1), 12 (2017).
[32]F. Troiani and M. Affronte, "Molecular spins for quantum information technologies," Chem. Soc. Rev. **40**, 3119–3129 (2011).
[33]M. Urdampilleta, S. Klyatskaya, J.-P. Cleuziou, M. Ruben, and W. Wernsdorfer, "Supramolecular spin valves," Nat. Mater. **10**, 502–506 (2011).
[34]M. Ganzhorn, S. Klyatskaya, M. Ruben, and W. Wernsdorfer, "Strong spin-photon coupling between a single-molecule magnet and a carbon nanotube nanoelectromechanical system," Nat. Nanotechnol. **8**, 165–169 (2013).
[35]S. Thiele, F. Balestro, R. Ballou, S. Klyatskaya, M. Ruben, and W. Wernsdorfer, "Electrically driven nuclear spin resonance in single-molecule magnets," Science **344**, 1135–1138 (2014).
[36]S. Lumetti, A. Candini, C. Godfrin, F. Balestro, W. Wernsdorfer, S. Klyatskaya, M. Ruben, and M. Affronte, "Single-molecule devices with graphene electrodes," Dalton Trans. **45**, 16570–16574 (2016).
[37]N. Ishikawa, M. Sugita, T. Okubo, N. Tanaka, T. Iino, and Y. Kaizu, "Determination of ligand-field parameters and f-electronic structures of double-decker bis(phthalocyaninato) lanthanide complexes," Inorg. Chem. **42**, 2440–2446 (2003).
[38]P. Zhu, F. Lu, N. Pan, D. P. Arnold, S. Zhang, and J. Jiang, "Comparative electrochemical study of unsubstituted and substituted bis(phthalocyaninato) rare earth (III) complexes," Eur. J. Inorg. Chem. **2004**, 510–517 (2004).
[39]N. Ishikawa, M. Sugita, and W. Wernsdorfer, "Quantum tunneling of magnetization in lanthanide single-molecular magnets bis(phthalocyaninato) terbium and bis(phthalocyaninato) dysprosium anions," Angew. Chem. Int. Ed. **44**, 2931–2935 (2005).
[40]L. Vitali, S. Fabris, A. M. Conte, S. Brink, M. Ruben, S. Baroni, and K. Kern, "Electronic structure of surface-supported bis(phthalocyaninato) terbium (III) single molecular magnets," Nano Lett. **8**, 3364–3368 (2008).
[41]M. Urdampilleta, S. Klyatskaya, M. Ruben, and W. Wernsdorfer, "Magnetic interaction between a radical spin and a single-molecule magnet in a molecular spin-valve," ACS Nano **9**, 4458–4464 (2015).
[42]S. Marocchi, A. Candini, D. Klar, W. Van den Heuvel, H. Huang, F. Troiani, V. Corradini, R. Biagi, V. De Renzi, S. Klyatskaya, K. Kummer, N. B. Brookes, M. Ruben, H. Wende, U. del Pennino, A. Soncini, M. Affronte, and V. Bellini, "Relay-like exchange mechanism through a spin radical between TbPc2 molecules and graphene/Ni(111) substrates," ACS Nano **10**, 9353–9360 (2016).
[43]F. Troiani, C. Godfrin, S. Thiele, F. Balestro, W. Wernsdorfer, S. Klyatskaya, M. Ruben, and M. Affronte, "Landau-Zener transition in a continuously measured single-molecule spin transistor," Phys. Rev. Lett. **118**, 257701 (2017).
[44]C. Godfrin, S. Thiele, A. Ferhat, S. Klyatskaya, M. Ruben, W. Wernsdorfer, and F. Balestro, "Electrical read-out of a single spin using an exchange-coupled quantum dot," ACS Nano **11**, 3984–3989 (2017).
[45]A. Abragam and B. Bleaney, *Electron Paramagnetic Resonance of Transition Ions* (Oxford University Press, 2012), ISBN: 0199651523.
[46]R. d. L. Kronig, "On the mechanism of paramagnetic relaxation," Physica **6**, 33–43 (1939).
[47]J. H. Van Vleck, "Paramagnetic relxation times for titanium and chrome alum," Phys. Rev. **57**, 426–447 (1940).
[48]R. Orbach, "Spin-lattice relaxation in rare-earth salts," Proc. R. Soc. A **264**, 458–484 (1961).
[49]M. Urdampilleta, "Spintronique moléculaire: de la vanne de spin à la detection d'un spin unique," Ph.D. thesis (Université Joseph Fourier, 2012), see https://tel.archives-ouvertes.fr/tel-00770488/file/30438_URDAMPILLETA_2012_archivage.pdf.